CrossMark

Augmented reality visualization: A review of civil infrastructure system applications

Amir H. Behzadan [a], Suyang Dong [b], Vineet R. Kamat [b],*

[a] Department of Civil, Environmental, and Construction Engineering, University of Central Florida, Orlando, FL 32816, USA
[b] Department of Civil and Environmental Engineering, University of Michigan, Ann Arbor, MI 48109, USA

ABSTRACT

In Civil Infrastructure System (CIS) applications, the requirement of blending synthetic and physical objects distinguishes Augmented Reality (AR) from other visualization technologies in three aspects: (1) it reinforces the connections between people and objects, and promotes engineers' appreciation about their working context; (2) it allows engineers to perform field tasks with the awareness of both the physical and synthetic environment; and (3) it offsets the significant cost of 3D Model Engineering by including the real world background. This paper reviews critical problems in AR and investigates technical approaches to address the fundamental challenges that prevent the technology from being usefully deployed in CIS applications, such as the alignment of virtual objects with the real environment continuously across time and space; blending of virtual entities with their real background faithfully to create a sustained illusion of co-existence; and the integration of these methods to a scalable and extensible computing AR framework that is openly accessible to the teaching and research community. The research findings have been evaluated in several challenging CIS applications where the potential of having a significant economic and social impact is high. Examples of validation test beds implemented include an AR visual excavator-utility collision avoidance system that enables workers to "see" buried utilities hidden under the ground surface, thus helping prevent accidental utility strikes; an AR post-disaster reconnaissance framework that enables building inspectors to rapidly evaluate and quantify structural damage sustained by buildings in seismic events such as earthquakes or blasts; and a tabletop collaborative AR visualization framework that allows multiple users to observe and interact with visual simulations of engineering processes.

© 2015 Elsevier Ltd. All rights reserved.

1. Introduction

In several science and engineering applications, visualization can enhance a user's cognition or learning experience and help communicate information about a complex phenomenon or to demonstrate the applicability of an abstract concept to real world circumstances. An important category of visualization is termed Virtual Reality (VR), which replaces the user's physical world with a totally synthetic environment and isolates the user's sensory receptors (eyes and ears) from the real physical world. The cost and effort of constructing a faithful synthetic environment includes tasks such as model engineering (the process of creating, refining,

archiving, and maintaining 3D models), scene management, and graphics rendering and can thus be enormous [1].

In contrast to VR, another category of visualization techniques, called Augmented Reality (AR), preserves the user's awareness of the real environment by compositing the real world and the virtual contents in a mixed (blended) 3D space [2]. For this purpose, AR must not only maintain a correct and consistent spatial relation between the virtual and real objects, but also sustain the illusion that they coexist in the augmented space. In addition, the awareness of the real environment in AR and the information conveyed by the virtual objects provide users with hints to discover their surroundings and help them perform real-world tasks [3]. Furthermore, AR offers a promising alternative to the model engineering challenge inherent in VR by only including entities that capture the essence of the study [4]. These essential entities usually exist in a complex and dynamic context that is necessary to the model, but costly to replicate in VR. However, reconstructing the context is rarely a problem in AR, where modelers can take full

* Corresponding author.
   E-mail addresses: amir.behzadan@ucf.edu (A.H. Behzadan), dsuyang@umich.edu (S. Dong), vkamat@umich.edu (V.R. Kamat).
   URLs: http://pegasus.cc.ucf.edu/~abehzada/ (A.H. Behzadan), http://pathfinder.engin.umich.edu (V.R. Kamat).

advantage of the real context (e.g., terrains and existing structures), and render them as backgrounds, thereby saving a considerable amount of effort and resources.

Fig. 1 shows the virtuality continuum, a concept first defined by Milgram and Kishino [5] that represents the mixture of classes of objects presented in any particular display situation. Within this continuum, the real environment (i.e., reality) and the virtual environment (i.e., VR) are shown at the two ends. While reality defines environments consisting solely of real objects, VR defines environments consisting solely of virtual objects, an example of which would be a conventional computer graphic simulation. As illustrated in this continuum, Mixed Reality (MR) is an environment in which real world and virtual world objects are presented together, that is, anywhere between the extremes of the virtuality continuum. AR and Augmented Virtuality (AV) fall in this category.

1.1. An overview of augmented reality in Architecture, Engineering, and Construction (AEC)

The application of visualization techniques such as AR for planning, analysis, and design of Architecture, Engineering, and Construction (AEC) projects is relatively new compared to the sizeable amount of AR-related research conducted for diverse applications in fields such as manufacturing, medical operations, military, and gaming. A thorough statistical review of recent AR-related research studies in AEC and potential future trends in this area was recently conducted by Rankohi and Waugh [6]. Their work showed that field workers and project managers have high interest in using non-immersive and desktop standalone AR technologies during project construction phase mainly to monitor progress and detect defective work. In another study, the potential of AR applications in AEC including eight work tasks (i.e., layout, excavation, positioning, inspection, coordination, supervision, commenting, and strategizing) was discussed [7]. A general overview of AR technology and its use in construction and civil engineering applications, as well as applications in other fields can be found in [8]. Examples of major undertakings in AR research and development that have at one point set the tone for future endeavors are provided in the following paragraphs. Section 1.2 will contain detailed discussions about more recent value-adding applications of AR within the AEC domain.

In order to assist with utility inspection and maintenance, researchers have used AR to visualize underground utilities, provide the ability to look beneath the ground, and inspect the subsurface utilities [9]. Some further exploration can be found in [10,11] where the work has been extended to improve visual perception for excavation safety and subsurface utilities, respectively. AR can serve as a useful inspection assistance method in the sense that it supplements a user's normal experience with context-related or geo-referenced virtual objects. For example, an AR system was developed by Webster et al. [12] for improving the inspection and renovation of architectural structures by allowing users to see columns behind a finished wall and re-bars inside the columns. A "discrepancy check" tool has been developed by Georgel et al. [13] that allows users to readily obtain an augmentation in order to find differences between an as-design 3D model and an as-built facility. Other researchers implemented a system for visualizing performance metrics that aims to represent progress deviations through the superimposition of 4D as-planned models over time-lapsed real jobsite photographs [14]. In another example, overlaying as-built drawings onto site photos for the purpose of continuous quality investigation of a bored pile construction was presented [15].

Some examples of coordinating and strategizing are the visualization of construction simulations and architectural designs. ARVISCOPE, an AR framework for visualization of simulated outdoor construction operations was designed by Behzadan and Kamat [16] to facilitate the verification and validation of the results generated by Discrete Event Simulation (DES). Another mobile AR platform called TINMITH2 was developed by Thomas et al. [17] and used to visualize the design of an extension to a building. Some other construction tasks which feature high complexity may also benefit from AR. For example, the quality of welding normally depends on the welders' experience and skill. By developing a welding helmet that augmented visual information such as paper drawings and online quality assistance, researchers were able to improve welders' working conditions as well as the quality control [18].

1.2. Recent advances in augmented reality for AEC applications

Recent applications of AR technology in AEC domain have helped improve performance in areas such as virtual site visits, comparing as-built and as-planned status of projects, preempting work package schedule disputes, enhancing collaboration opportunities, and planning and training for similar projects [6,19]. Examples of such application areas include but are not limited to a framework for analyzing, visualizing, and assessing architectural/construction progress with unordered photo collections and 3D building models [20,21], a client/server AR system for viewing complex assembly models on mobile phones [22], a tangible MR-based virtual design prototype as a distributed virtual environment (DVE) for the purpose of improving remote design review collaboration [23], an AR interior design service which combines features of social media, AR and 3D modeling to ambient home design [24], an interactive speech and gesture recognition-based, immersive AR model designed to visualize and interact with buildings and their thermal environments [25], an integrated AR-based framework for indoor thermal performance data visualization that utilizes a mobile robot to generate environment maps [26], a tabletop AR system for collaboratively visualizing computer-generated models [27], and a mobile AR application capable of delivering context-aware visual project information to students and trainees to improve the quality and pace of learning [28].

The Laboratory for Interactive Visualization in Engineering (LIVE) at the University of Michigan has been engaged in AR research with applications related to construction operations planning, inspection, safety, and education. These AEC applications include visual excavator-collision avoidance systems, rapid reconnaissance systems for measuring earthquake-induced building damage, and visualization of operations-level construction processes in both outdoor AR and the collaborative tabletop AR environments (Fig. 2). The developed visual collision avoidance system allows excavator operators to persistently "see" what utilities lie buried in the vicinity of a digging machine or a human spotter, thus helping prevent accidents caused by utility strikes [29]. With the aid of AR, the rapid post-disaster reconnaissance system for building damage assessment superimposes previously stored building baselines onto the corresponding images of a real structure. The on-site inspectors can then estimate the damage by evaluating discrepancies between the baselines and the real building edges [30]. Moreover, research was conducted to enable the visualization of construction operations in outdoor AR to facilitate the
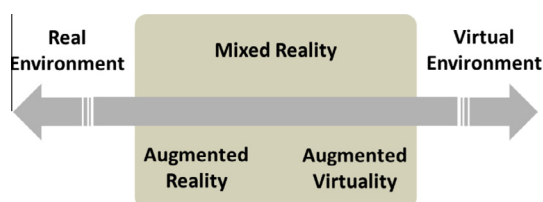

Fig. 1. Milgram's virtuality continuum.

Visual Collision-Avoidance
[29]

Reconnaissance of Damaged Building
[30]

Visualization of Construction Processes
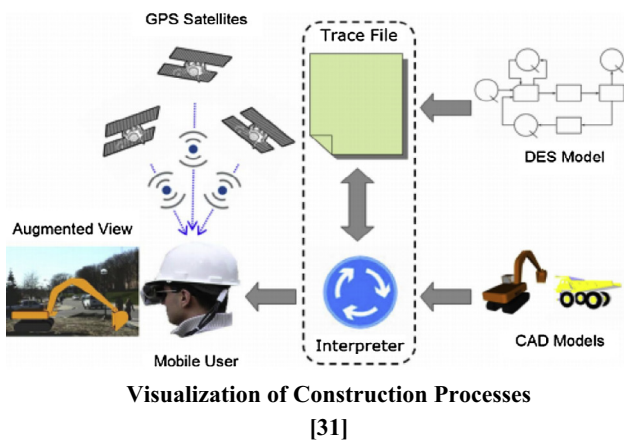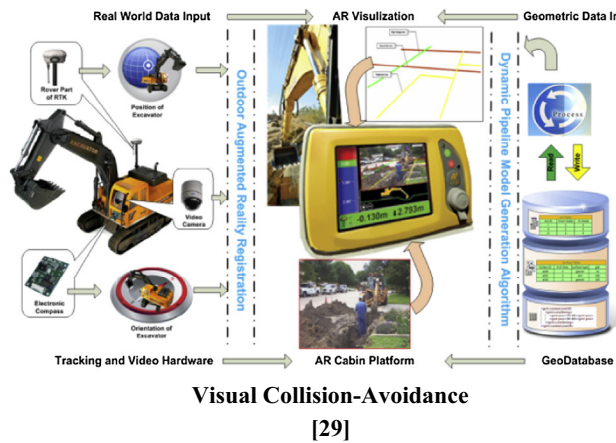**[31]**

Collaborative AR Visualization
[27]

Fig. 2. AR research for AEC applications in LIVE.

verification and validation of the results of simulated construction processes, with minimum effort spent on creating 3D models of the surrounding environment [31]. Lastly, the tabletop collaborative AR visualization helps to bridge the gap between paper-based static information and computer-based graphical models. It reflects the dynamic nature of a jobsite, and preserves the convenience of face-to-face collaboration [27].

2. Challenges associated with AR in AEC applications

In this Section, key challenges associated with AR research and development are discussed in detail. The main focus of the following Subsections will be on spatial alignment of real and virtual entities (a.k.a. registration), and visual illusion of virtual and real world coexistence (a.k.a. occlusion) both have been identified throughout the literature as key design and implementation issues [2]. It must be noted that the development of AR tools with specific applications in civil infrastructure may introduce other challenges such as mobility and ergonomics, ruggedness (ability to function in chaotic and harsh environments), power limitations, and adverse weather conditions. However, such challenges are technology-specific and therefore, are not within the direct scope of this paper.

2.1. Spatial alignment of real and virtual entities (registration)

The goal of spatial registration in AR is to properly align real world objects and superimposed virtual objects with respect to each other [16]. Without proper registration, the illusion that the two worlds coexist inside the augmented space will be
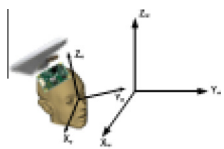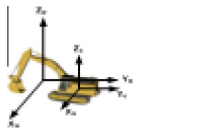
compromised. As shown in Table 1, the registration process typically consists of four major steps [32]:

1. Positioning the viewing volume of a user's eyes in the world coordinate system.
2. Positioning virtual objects in the world coordinate system.
3. Determining the shape of the viewing volume.
4. Converting virtual objects from the world coordinate system to the eye coordinate system.

Since the origin of the world coordinate system coincides with the user's eye coordinate system, which is the user's geographical location in each frame, these steps must consider 6 degrees of freedom (3 for position and 3 for head orientation) measured by tracking devices, as well as the lens parameters of the camera that captures the real world views. As shown in Fig. 3, the world coordinate system uses a right-handed system with the Y-axis pointing in the direction of the true north, the X-axis pointing to the east, and the Z-axis pointing upward. The eye coordinate system complies with the OpenSceneGraph (OSG) [33] default coordinate system, using a right-handed system with the Z-axis as the up vector, and the Y-axis departing from the eye.

As shown in Fig. 3, the yaw, pitch, and roll angles are used to describe the relative orientation between the world and eye coordinate systems. The zxy rotation sequence is picked to construct the transformation matrix between the two coordinate systems. Suppose the eye and world coordinate systems coincide at the beginning. The user's head rotates around the Z-axis by yaw angle $\Psi \in (-180, +180]$ to get the new axes, X' and Y'. Since the

Table 1
The four steps of the registration process in AR.

| Step	Task	Illustration	Parameters and device
Viewing	Position the viewing volume of a user's eyes in the world		Attitude of the camera (Electronic Compass)
Modeling	Position the objects in the world		Location of the world origin (RTK GPS)
Creating viewing frustum	Decide the shape of the viewing volume		Lens and aspect ratio of camera (Camera)
Projection	Project the objects onto the image plane		Perspective projection matrix
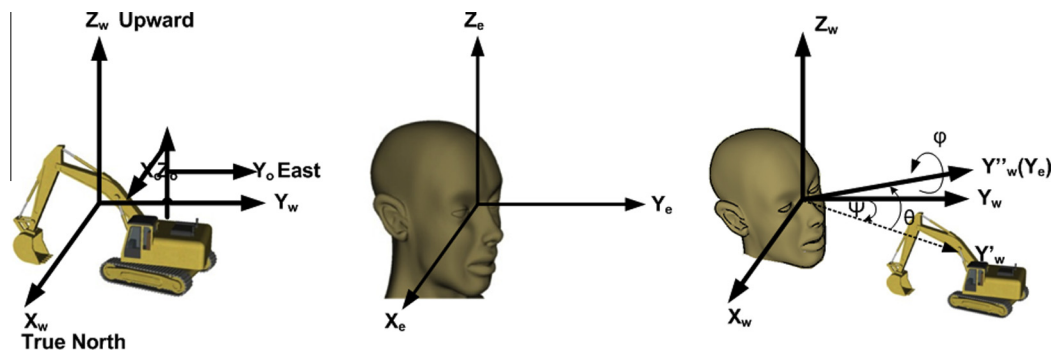
Fig. 3. Definition of the world coordinate system.

rotation is clockwise under the right-handed system, the rotation matrix is $R_z(-\Psi)$. Secondly, the head rotates around the X'-axis by pitch angle $\Theta \in [-90, +90]$ to get the new axes Y'' and Z'', with counter-clockwise rotation of $R_{x'}(\Theta)$. Finally, the head rotates around the Y''-axis by roll angle $\Phi \in (-180, +180]$ with a counter-clockwise rotation of $R_{y''}(\Phi)$ to reach the final attitude.

Converting the virtual object from the world coordinate (P_w) to the eye coordinate (P_e) is an inverse process of rotating from the world coordinate system to the eye coordinate system, therefore the rotating matrix is written as $R_z(\Psi)R_{x'}(-\Theta)R_{y''}(-\Phi)$, as shown in Eq. (1). Since OSG provides quaternion, a simple and robust way to express rotation, the rotation matrix is further constructed as quaternion by specifying the rotation axis and angles. The procedure is explained as follows, and all associated equations are listed in sequence in Eqs. (2)–(5): rotating around the Y''-axis by $-\Phi$ degrees, then rotating around the X'-axis by $-\Theta$ degrees, and finally rotating around the Z-axis by Ψ degrees.

$$
\begin{bmatrix} X_e \\ Y_e \\ Z_e \end{bmatrix} = \begin{bmatrix} \cos(\Psi) & \sin(-\Psi) & 0 \\ \sin(\Psi) & \cos(\Psi) & 0 \\ 0 & 0 & 1 \end{bmatrix} * \begin{bmatrix} 1 & 0 & 0 \\ 0 & \cos(\Theta) & \sin(\Theta) \\ 0 & \sin(-\Theta) & \cos(\Theta) \end{bmatrix}
$$
$$
* \begin{bmatrix} \cos(\Phi) & 0 & \sin(-\Phi) \\ 0 & 1 & 0 \\ \sin(\Phi) & 0 & \cos(\Phi) \end{bmatrix} * \begin{bmatrix} X_w \\ Y_w \\ Z_w \end{bmatrix} \tag{1}
$$

$$
P_e = R_z(\Psi) * R_{x'}(-\Theta) * R_{y''}(-\Phi) * P_w \tag{2}
$$

$$
Z\text{-}axis = \begin{bmatrix} 0 \\ 0 \\ 1 \end{bmatrix} \tag{3}
$$

$$
X'\text{-}axis = \begin{bmatrix} \cos(\Psi) & \sin(\Psi) & 0 \\ \sin(-\Psi) & \cos(\Psi) & 0 \\ 0 & 0 & 1 \end{bmatrix} * \begin{bmatrix} 1 \\ 0 \\ 0 \end{bmatrix} = \begin{bmatrix} \cos(\Psi) \\ -\sin(\Psi) \\ 0 \end{bmatrix} \tag{4}
$$

$$
Y''\text{-}axis = \begin{bmatrix} 1 & 0 & 0 \\ 0 & \cos(\Theta) & \sin(-\Theta) \\ 0 & \sin(\Theta) & \cos(\Theta) \end{bmatrix} * \begin{bmatrix} \cos(\Psi) & \sin(\Psi) & 0 \\ \sin(-\Psi) & \cos(\Psi) & 0 \\ 0 & 0 & 1 \end{bmatrix}
$$
$$
* \begin{bmatrix} 0 \\ 1 \\ 0 \end{bmatrix} = \begin{bmatrix} \sin(\Psi) \\ \cos(\Theta)\cos(\Psi) \\ \sin(\Theta)\cos(\Psi) \end{bmatrix} \tag{5}
$$

Once the rotation sequence and transformation is completed, the next step is to model the virtual objects in their exact locations. The definition of the object coordinate system is determined by the drawing software. The origin is fixed to a pivot point on the object with user-specified geographical location. The geographical
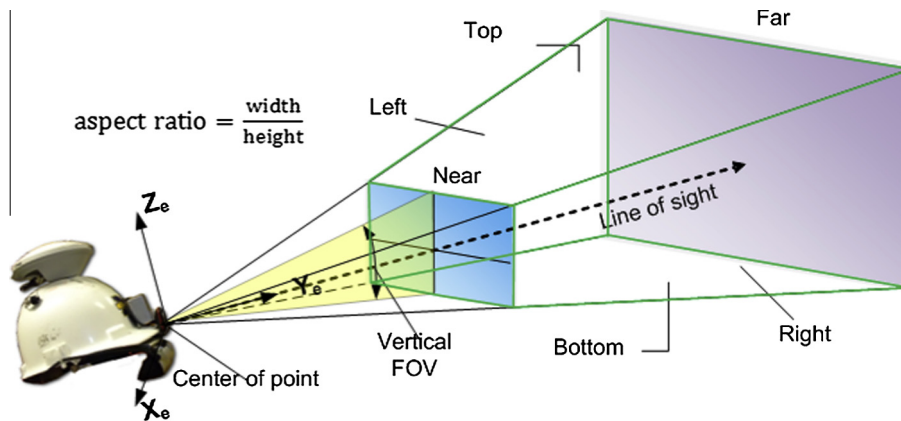
Fig. 4. The viewing frustum defines the virtual content that can be seen.

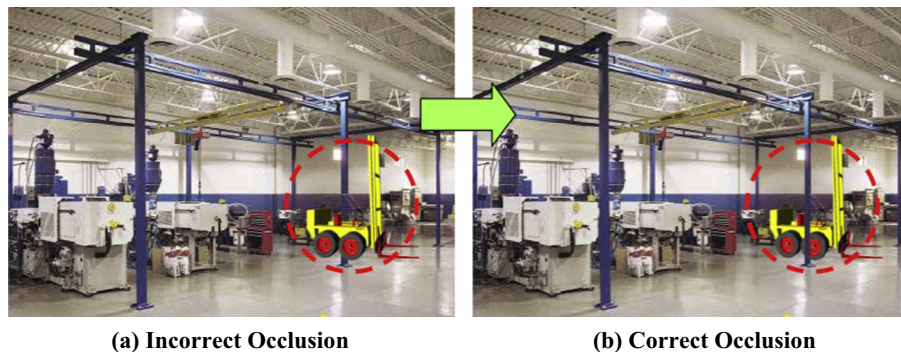**(a) Incorrect Occlusion**

(b) Correct Occlusion

Fig. 5. Example of incorrect and correct occlusion in AR visualization.

location of the world coordinate origin is also given by position tracking devices (e.g., GPS sensor) carried by the user. Therefore, a 3D vector between the object and world coordinate origins can be calculated. The methods to calculate the distance between geographical coordinates is originally introduced by Vincenty [34] and later used by Behzadan and Kamat [16] to design an inverse method that uses a reference point to calculate the 3D distance vector between two geographical locations. Once a virtual object is modeled inside the user's viewing frustum, future translation, rotation, and scaling operations can be easily applied to that object.

Finally, the user's viewing frustum must be defined. The real world is perceived through the perspective projection by the human eye and the video camera. Four parameters are needed to construct a perspective projection matrix: horizontal angle of view, horizontal and vertical aspect ratio, and near and far planes. As shown in Fig. 4, these parameters together form a viewing frustum and determine which virtual content should be displayed in the augmented space. In order to increase computational efficiency, all virtual objects outside the viewing frustum are either cropped or clipped.

2.2. Visual illusion of virtual and real world coexistence (occlusion)

In an ideal AR visualization, real and virtual objects must be seamlessly blended in all three dimensions. The result of composing an AR scene without considering the relative depth of the real and virtual objects (which is the case in most current AR approaches) is that the graphical entities in the scene appear to "float" over the real background, rather than blend or coexist with real objects in that scene. This phenomenon is commonly referred to as incorrect occlusion. The occlusion problem is more complicated in outdoor AR where the user expects to navigate the space

freely, and where the relative depth between the virtual and real contents changes over time. Fig. 5 is a schematic AR scene where a real structural column is closer than a virtual forklift to the viewpoint [35]. The right-side image shows visually correct occlusion where the forklift is partially blocked by the structural column. The left-side image shows the same scene with incorrect illusion where the forklift appears to be in front of the column.

Several researchers have explored the AR occlusion problem from different perspectives. For example, a fast-speed stereo matching algorithm was implemented that infers depth maps from a stereo pair of intensity bitmaps [36]. However, random gross errors blink virtual objects on and off and turn out to be very distracting. In another study, a contour-based approach was proposed but with the major limitation that the contours need to be seen from frame to frame [37]. Later, this approach was refined with a semi-automated approach that requires the user to outline the occluding objects in the key-views, and then the system automatically detects these occluding objects and handles uncertainties on the computed motion between two key frames [38]. Despite the visual improvements, the semi-automated method is only appropriate for post-processing. In another study, a model-based approach using a bounding box, and a depth-based approach using a stereo camera were investigated [39]. The former works only with a static viewpoint and the latter is subject to low-textured areas. Also, researchers in [40,41] tried to increase the accuracy of the depth map by a region of interest extraction method using background subtraction and stereo depth algorithms. However, only simple background examples were demonstrated. In a separate effort, an interactive segmentation and object tracking method was designed for real-time occlusion, but this algorithm failed in situations where virtual objects are in front of the real objects [42].

In the authors' research, a robust AR occlusion algorithm was designed and implemented that uses a real-time Time-of-flight (TOF) camera, an RGB video camera, OpenGL Shading Language (GLSL), and render to texture (RTT) techniques to correctly resolve the depth of real and virtual objects in real-time AR visualizations. Compared to previous work, this approach enables improvements in three ways:

1. *Ubiquity:* The TOF camera is capable of suppressing background illumination and enables the designed algorithm to work in both indoor and outdoor environments. It puts the least limitation on context and conditions compared with previous approaches.
2. *Robustness:* Using the OpenGL depth-buffering method, it can work regardless of the spatial relationship among involved virtual and real objects.
3. *Speed:* The processing and sampling of the depth map is parallelized by taking advantage of the GLSL fragment shader and the RTT technique. A parallel research effort was described by Koch et al. [43] that adopted a similar approach for TV production in indoor environments with a 3D model constructed beforehand with the goal of segmenting a moving actor from the background.

A fundamental step to correct occlusion handling is obtaining an accurate measurement of the distance from the virtual and real object to the user's eye. In an outdoor AR environment, the metric distance between a virtual object and the viewpoint with known geographical locations can be calculated using the Vincenty algorithm [34]. In a simulated construction operation, for example, the geographical locations of virtual building components and equipment can be extracted from the engineering drawings. The location of the viewpoint, on the other hand, is tracked by a high-accuracy position sensor (e.g., Real-Time Kinematics (RTK)-enabled GPS receiver with centimeter-level accuracy) carried by the user. A TOF camera (with a range enough to cover the immediate space in front of an AR user) estimates the distance from the real object to the eye using the time-of-flight principle, which measures the time that a signal travels, with well-defined speed, from the transmitter to the receiver [44].

Specifically, the TOF camera measures radio frequency (RF)-modulated light sources with phase detectors. The modulated outgoing beam is sent out with an RF carrier, and the phase shift of that carrier is measured on the receiver side to compute the distance [45]. Compared to traditional light detection and ranging (LIDAR) scanners and stereo vision, the TOF camera features real-time feedback with high accuracy. It is capable of capturing a complete scene with one shot, and with speeds of up to 40 frames per second (fps). However, common TOF cameras are vulnerable to background light (e.g., artificial lighting and the sun) that generates electrons as this confuses the receiver. In the authors' research, the suppression of background illumination (SBI) method is used to allow the TOF camera to work flexibly in both indoor and outdoor environments [30].

2.2.1. Two-stage rendering

Depth buffering, also known as *z*-buffering, is the solution for hidden-surface elimination in OpenGL, and is usually done efficiently in the graphics processing unit (GPU). A depth buffer is a 2D array that shares the same resolution with the color buffer and the viewport. If enabled in the OpenGL drawing stage, the depth buffer keeps record of the closest depth value to the observer for each pixel. For an incoming fragment at a certain pixel, the fragment will not be drawn unless its corresponding depth value is smaller than the previous one. If it is drawn, then the corresponding depth value in the depth buffer is replaced by the smaller one.

In this way, after the entire scene has been drawn, only those fragments that were not obscured by any others remain visible.

Depth buffering thus provides a promising approach for solving the AR occlusion problem. Fig. 6 shows a two-stage rendering method. In the first rendering stage, the background of the real scene is drawn as usual, but with the depth map retrieved from the TOF camera written into the depth buffer at the same time. In the second stage, the virtual objects are drawn with depth buffer testing enabled. Consequently, the invisible part of virtual object, either hidden by a real object or another virtual one, will be correctly occluded.

2.2.2. Implementation challenges

Despite the straightforward implementation of depth buffering, there are several challenges when integrating the depth buffer with the depth map from the TOF camera:

1. After being processed through the OpenGL graphics pipeline and written into the depth buffer, the distance between the OpenGL camera and the virtual object is no longer the physical distance [32]. The transformation model is explained in Table 2. Therefore, the distance for each pixel from the real object to the viewpoint recorded by the TOF camera has to be processed by the same transformation model, before it is written into the depth buffer for comparison.
2. There are three cameras for rendering an AR space: A video camera, a TOF camera, and an OpenGL camera. The video camera captures RGB or intensity values of the real scene as the background, and its result is written into the color buffer. The TOF camera acquires the depth map of the real scene, and its result is written into the depth buffer. The OpenGL camera projects virtual objects on top of real scenes, with its result being written into both the color and depth buffers. In order to ensure correct alignment and occlusion, ideally all cameras should share the same projection parameters (the principle points and focal lengths). Even though the TOF camera provides an integrated intensity image that can be aligned with the depth map by itself, the monocular color channel compromises the visual credibility. On the other hand, if an external video camera is used, then the intrinsic and extrinsic parameters of the video camera and TOF camera may not agree (i.e., different principle points, focal lengths, and distortions). Therefore, some image registration methods are required to find the correspondence between the depth map and the RGB image. A detailed description of both methods including a non-linear homography estimation implementation adopted from [46] and stereo projection that are used to register the depth map and RGB image can be found in [30]. The projection parameters of OpenGL camera are adjustable and can accommodate either an RGB or TOF camera. Fig. 7 shows snapshots of the occlusion effect achieved in the authors' research by using homography mapping between the TOF camera and the RGB camera.
3. Traditional OpenGL pixel-drawing commands can be extremely slow when writing a 2D array (i.e., the depth map) into the frame buffer. In this research, an alternative and efficient approach using OpenGL texture and GLSL is used.
4. The resolution of the TOF depth map is fixed as 200×200, while that of the depth buffer can be arbitrary, depending on the resolution of the viewport. This implies the necessity of interpolation between the TOF depth map and the depth buffer. Furthermore, image registration demands an expensive computation budget if a high-resolution viewport is defined. In this research, the RTT technique is used to carry out the interpolation and registration computation in parallel.
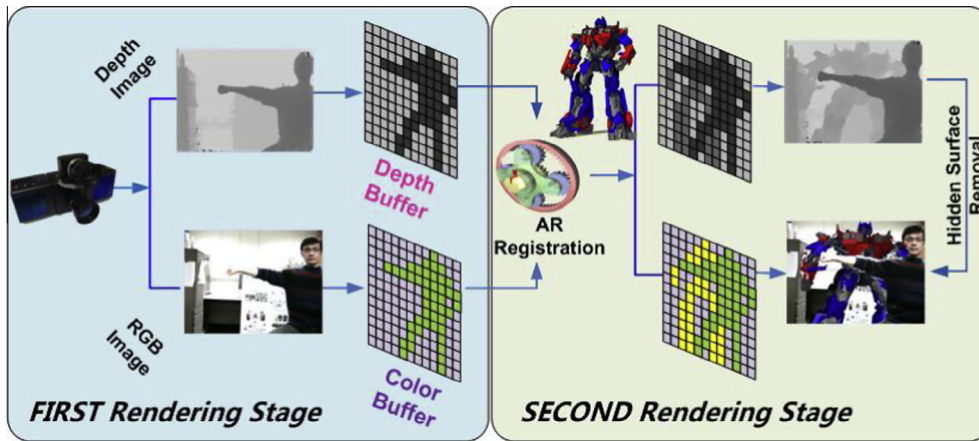
Fig. 6. Two-stage rendering for occlusion handling.

Table 2
The transformation steps applied to the raw TOF depth image.

Name	Meaning	Operation	Expression	Range
Z_e	Distance to the viewpoint	Acquired by TOF camera		$(0, +\infty)$
Z_c	Clip coordinate after projection transformation	$M_{\text{ortho}} * M_{\text{perspective}} * [X_e\ Y_e\ Z_e\ W_e]^T$	$Z_c = \frac{Z_e*(f+n)}{f-n} - \frac{2*f*n*W_e}{f-n}$ n and f are the near and far planes, W_e is the homogenous component in eye coordinate, and is usually equal to 1	$[-n, f]$
Z_{cvv}	Canonical view volume	Z_c/W_c ($W_c = Z_e$, and is the homogenous component in clip coordinate)	$Z_{cvv} = \frac{f+n}{f-n} - \frac{2*f*n}{Z_e*(f-n)}$	$[-1, 1]$
Z_d	Value sent to depth buffer	$(Z_{ndc} + 1)/2$	$Z_d = \frac{f+n}{2*(f-n)} - \frac{f*n}{Z_e*(f-n)} + 0.5$	$[0, 1]$

Fig. 7. Occlusion effect comparison using homography mapping between the TOF camera and the RGB camera.

3. Software and hardware for AR in AEC applications

In this Section, design and implementation issues associated with the AR applications and prototypes developed by LIVE researchers at the University of Michigan are presented and discussed. The software- and hardware-related problems identified and addressed in LIVE were mainly motivated by three specific needs of mobility, extensibility, and scalability, which are often considered as prohibiting factors in the application of AR in civil infrastructure. It must be noted that research and development efforts that aim to address these issues are still ongoing and even the majority of existing commercial AR applications have not yet completely developed to fully address all such problems in one application. For instance, Bentley Systems has recently introduced its first prototype of a simplified augmentation environment to overlay 2D drawing information on static panoramic images.

While this approach offers jitter-free augmentation, there is no live video tracking or real-time augmentation, and the images are by definition, out of date [47]. The following Subsections provide useful insight for future AR software and hardware design and improvement efforts.

3.1. Software interfaces

SMART (acronym for Scalable and Modular Augmented Reality Template) is an extensible AR computing framework that is designed to deliver high-accuracy and convincing augmented graphics that correctly place virtual contents relative to a real scene, and robustly resolve the occlusion relationships between them [48]. SMART is built on top of the previously designed ARVISCOPE platform [8] and is a loosely coupled interface that is independent of any specific engineering application or domain. Instead, it can be readily adapted to an array of engineering applications such as visual collision avoidance of underground facilities, post-disaster reconnaissance of damaged buildings, and visualization of simulated construction processes. The in-built registration algorithm of SMART guarantees high-accuracy static alignment between real and virtual objects. Some efforts have also been made to reduce dynamical misregistration, including:

1. In order to reduce synchronization latency, multiple threads are dynamically generated for reading and processing sensor measurement immediately upon the data arrival in the host system.
2. The FIR filter applied to jittering output of the electronic compass leads to filter-induced latency, therefore an adaptive lag compensation algorithm is designed to eliminate the dynamic misregistration.

The SMART framework follows the classical model-view-controller (MVC) pattern. Scene-Graph-Controller is the implementation of the MVC pattern in SMART, and is described below:

1. The model counterpart in SMART is the scene that utilizes application-specific input/output (I/O) engines to load virtual objects, and that maintains their spatial and attribute status. The update of a virtual object's status is reflected when it is time to refresh the associated graphs.
2. The graph corresponds to the view and reflects the AR registration results for each frame update event. Given the fact that the user's head can be in continuous motion, the graph always invokes callbacks to rebuild the transformation matrix based on the latest position and attitude measurement, and refreshes the background image.
3. The controller manages all user interface (UI) elements, and responds to a user's commands by invoking delegates' member functions such as a scene or a graph.

The framework of SMART that is based on a Scene-Graph-Controller set-up is shown in Fig. 8 and is constructed in the following way: the main entry of the program is `CARApp`, which is in charge of `CARSensorForeman` and `CARSiteForeman`. The former initializes and manages all of the tracking devices such as RTK GPS receivers and electronic compasses, while the latter defines the relation among scene, graphs, and controller. Once a `CARSiteForeman` object is initialized, it orchestrates the creation of `CARScene`, `CARController`, and `CARGraph`, and the connection of graphs to the appropriate scene [48]. Applications derived from SMART are Single Document Interface (SDI). Therefore, there is only one open scene and one controller within a `SmartSite`. The controller keeps pointers to the graph and the scene.

3.2. Hardware platforms

The designed software interface must be accompanied by a robust and easy-to-deploy hardware platform that enables users to perform operations in both indoor and outdoor settings. ARMOR (acronym for Augmented Reality Mobile Operation platform) evolves from the UM-AR-GPS-ROVER platform [49].
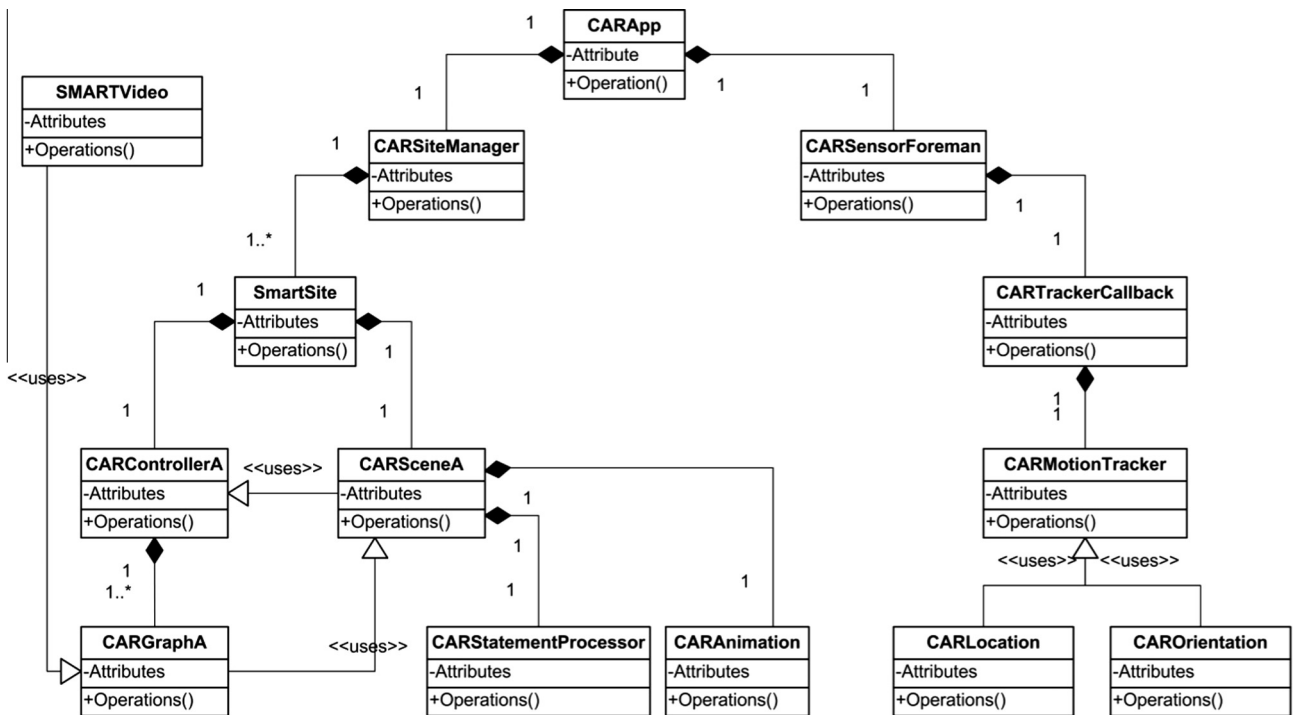

Fig. 8. SMART framework architecture.

Table 3
Comparison between UM-AR-GPS-ROVER and ARMOR platforms.

| Component	UM-AR-GPS-ROVER	ARMOR	Comparison
Location tracking	Trimble AgGPS 332 using OmniStar XP correction for Differential GPS method	Trimble AgGPS 332 using CMR correction broadcast by a Trimble AgGPS RTK Base 450/900	OmniStar XP provides 10–20 cm accuracy. RTK provides 2.5 cm horizontal accuracy, and 3.7 cm vertical accuracy
Orientation tracking	PNI TCM 5	PNI TCM XB	Same accuracy, but ARMOR places TCM XB rigidly close to camera
Video camera	Fire-I Digital Firewire Camera	Microsoft LifeCam VX-5000	LifeCam VX-5000 is lightweight, has small volume, and uses less wire
Head-mounted display	i-Glasses SVGA Pro video see-through HMD	eMagin Z800 3DVisor	Z800 3DVisor is lightweight with stereovision
Laptop	Dell Precision M60 Notebook	ASUS N10J Netbook	ASUS N10J is lightweight, has small volume, and is equipped with NVIDIA GPU
User command input	WristPC wearable keyboard and Cirque Smart Cat touchpad	Nintendo Wii Remote	Wii Remote is lightweight and intuitive to use
Power source	Fedco POWERBASE	Tekkeon myPower MP3750	MP3750 is lightweight and has multiple voltage outputs charging both GPS receiver and HMD
Backpack apparatus	Kensington Contour Laptop Backpack	Load Bearing Vest	Extensible and easy to access equipment
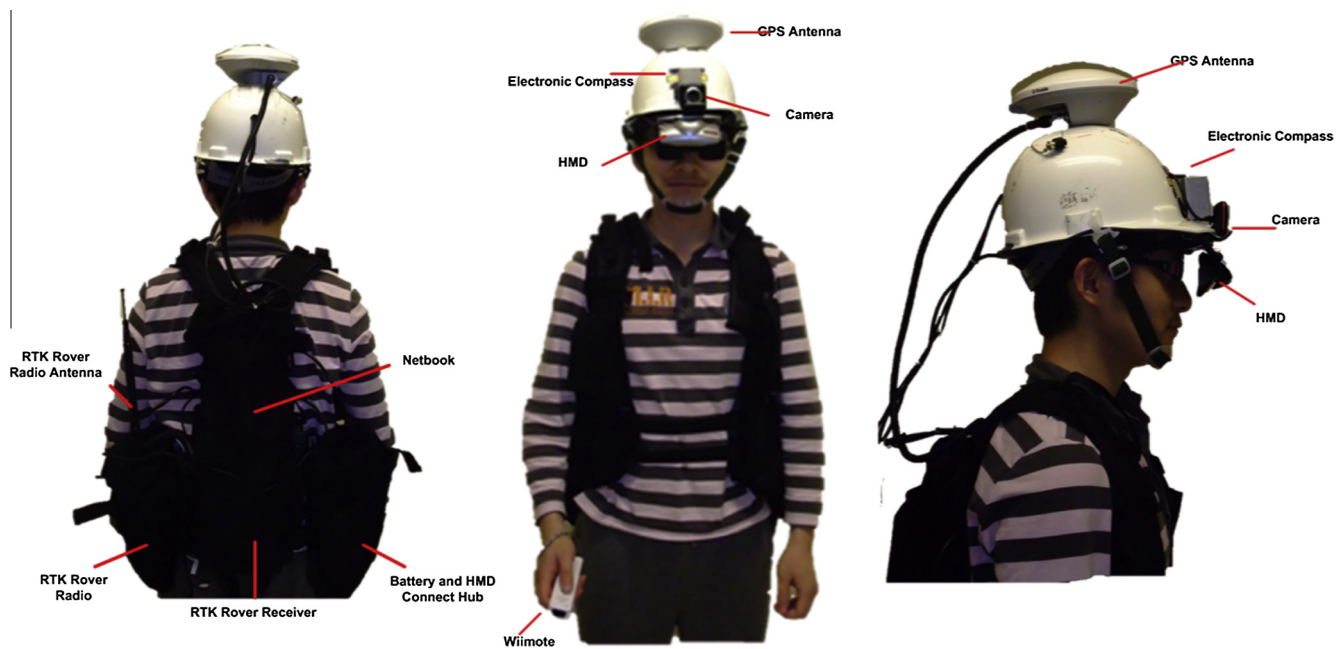
Fig. 9. The profile of ARMOR from different perspectives.

ARMOR introduces high-accuracy and lightweight devices, rigidly places all tracking instruments with full calibration, and renovates the carrying harness to make it more wearable. The improvements featured in ARMOR can be broken into four categories:

1. Highly accurate tracking devices with rigid placement and full calibration.
2. Lightweight selection of I/O and computing devices and external power source.
3. Intuitive user command input.
4. Load-bearing vest to accommodate devices and distribute weight evenly around the body.

An overview comparison between UM-AR-GPS-ROVER and ARMOR is listed in Table 3.

ARMOR can work in both indoor and outdoor modes. The indoor mode does not necessarily imply that the GPS signal is unavailable, but that the qualified GPS signal is absent. The GPS signal quality can be extracted from the $GGA section of the GPS data string that follows the National Marine Electronics Association (NMEA) format. The fix quality ranges from 0 to 8. For example, 2 means

differential GPS (DGPS) fix, 4 means RTD fix, and 5 means float RTK. The user can define the standard (i.e., which fix quality is deemed as qualified) in the hardware configuration file. When a qualified GPS signal is available, the geographical location is extracted from the $GPGGA section of the GPS data string. Otherwise, a preset pseudo-location is used, and this pseudo-location can be controlled by a keyboard.

The optimization of all devices in aspects such as volume, weight, and rigidity allows that all components be compacted and secured into one load-bearing vest. Fig. 9 shows the configuration of the ARMOR backpack and the allocation of hardware. There are three primary pouches: the back pouch accommodates the AgGPS 332 Receiver, the SiteNet 900 is stored in the right side pouch, and the left-side pouch holds the HMD connect interface box to a PC and the MP3750 battery. An ASUS N10J netbook is securely tied to the inner part of the back. All other miscellaneous accessories (e.g., USB to serial port hubs, AAA batteries) are distributed in the auxiliary pouches. The wire lengths are customized to the vest, which minimizes outside exposure. The configuration of the vest has several advantages over the Kensington Contour laptop backpack used by ARVISCOPE. First, the design of the

Fig. 10. Schematic overview of the designed AR-assisted assessment methodology.

pouches allows for an even distribution of weight around the body. Second, the separation of devices allows the user to conveniently access and checks the condition of certain hardware. Third, different parts of the loading vest are loosely joined so that the vest can fit any body type, and be worn rapidly even when fully loaded. ARMOR has been tested by several users for outdoor operation that lasted for over 30 continuous minutes, without any interruption or reported discomfort.

4. Implemented AEC applications

4.1. Augmented reality-assisted building damage reconnaissance

Following a major seismic event, rapid and accurate evaluation of a building condition is essential for determining its structural integrity for future occupancy. Current inspection practices usually conform to the ATC-20 post-earthquake safety evaluation field manual and its addendum, which provide procedures and guidelines for making on-site evaluations [50]. Responders (i.e., inspectors, structural engineers, and other specialists) often conduct visual inspections and designate affected buildings as green (apparently safe), yellow (limited entry), or red (unsafe) for immediate occupancy [51]. However, this approach is slow and often subjective and thus may sometimes suffer from misinterpretation, especially given that building inspectors do not have enough opportunities to conduct building safety assessments and verify their judgments, as earthquakes are infrequent [52–54]. In light of this, researchers have been proposing quantitative measurement most of which build on the premise that significant local structural damage manifests itself as translational displacement between consecutive floors, which is referred to as the inter-story drift [55]. The inter-story drift ratio (IDR), which is the inter-story drift divided by the height of the story, is a critical structural performance indicator that correlates the exterior deformation with the internal structural damage. For example, a peak IDR larger than 0.025 signals the possibility of a serious threat to human safety, and values larger than 0.06 translate to severe damage [56].

Calculating the IDR commonly follows contact (specifically the double integration of acceleration) or non-contact (vision-based or laser scanning) methods. It has been stated that he double

integration method may not be well suited for nonlinear responses due to sparse instrumentation or subjective choices of signal processing filters [57]. On the other hand, most vision-based approaches require the pre-installation of a target panel or emitting light source which may not be widely available and can be subject to damage during long-term maintenance [58–62].

A methodology to projecting the previously stored building baseline onto the real structure, and using a quantitative method to count the pixel offset between the augmented baseline and the building edge was first proposed by Kamat and El-Tawil [54]. Despite the stability of this method, it required a carefully aligned perpendicular line of sight from the camera to the wall for pixel counting. Such orthogonal alignment becomes unrealistic for high-rise buildings, since it demands the camera and the wall to be at the same height. Later, Dai et al. [15] removed the premise of orthogonality using a photogrammetry-assisted quantification method, which established a projection relation between 2D photo images and the 3D object space. However, the issue of automatic edge detection and the feasibility of deploying such a method at large scales, for example with high-rise buildings, have not been addressed.

In this Subsection, a new algorithm called line segment detector (LSD) for automating edge extraction, as well as a new computational framework for automating the damage detection procedure are introduced. In order to verify the effectiveness of these methods, a synthetic virtual prototyping (VP) environment was designed to profile the detection algorithm's sensitivity to errors inherent in the used tracking devices. Fig. 10 shows the schematic overview of measuring earthquake-induced damage manifested as a detectable drift in a building's façade. The previously stored building information is retrieved and superimposed as a baseline wireframe image on the real building structure after the damage. The sustained damage can be then evaluated by comparing the key differences between the augmented baseline and the actual drifting building edge. Fig. 10 also demonstrates the hardware prototype ARMOR [63] on which the developed application can be deployed. The inspector wears a GPS antenna and a RTK radio that communicates with the RTK base station. Together they can track the inspector's position up to centimeter-accuracy level. The estimation procedure and the final results can be shown in an HMD to the inspector.
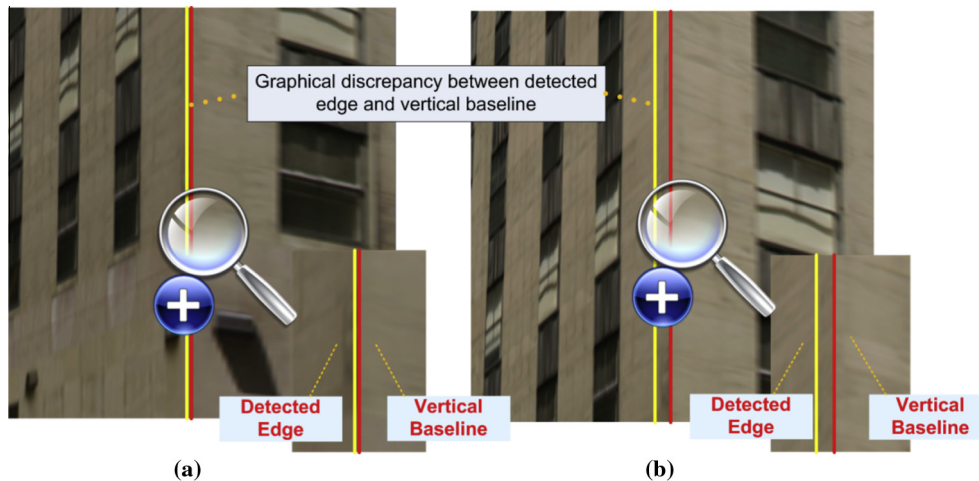
Fig. 11. Graphical discrepancy between the vertical baseline and the detected building edge provides hints about the magnitude of the local damage.
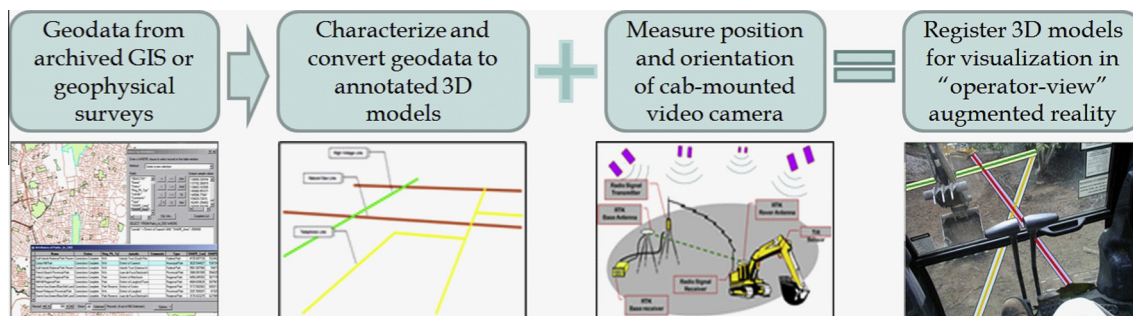

Fig. 12. Overview of the designed approach for visualization of buried asset geodata in operator-view AR.

Besides being a quantitative means of providing reliable damage estimation results, the vertical baseline of the building structure is also a qualitative alternative for visual inspection of local damage. By observing the graphical discrepancy between the vertical baseline and the real building edge, the on-site reconnaissance team can approximately but quickly assess how severe the local damage is in the neighborhood of the visual field. In other words, the larger the graphical discrepancy, the more severe the damage. The two snapshots of Fig. 11 focus on different key locations of the building, but they are taken from the same angle (i.e., direction). The bottom-right window on each image is a zoom-in view of the key location. The two vertical lines in the zoom-in window represent the detected edge and the vertical baseline, respectively. The fact that the gap between the detected edge and the vertical baseline in Fig. 11(a) is smaller than that of Fig. 11(b) indicates that the key location in Fig. 11(b) suffered more local damage than that of Fig. 11(a).

The experimental results with ground true location and orientation data were proven to be satisfactory for damage detection requirements. The results also highlighted the conditions for achieving the ideal measurement accuracy, for example observing distance, angle, and image resolution. The experimental results with instrumental errors reveal the bottleneck in field implementation. While the state-of-the-art RTK-GPS sensor can meet the location accuracy requirement, the electronic compass is not accurate enough to supply qualified measurement data, suggesting that alternative survey-grade orientation measurement methods must be identified to replace electronic compasses. The conducted sensitivity analysis developed a clear matrix revealing the relationship between instrument accuracy and accuracy of computed drift,

so the practical implementation of the proposed method can evolve with choices made for higher-accuracy instruments than the ones tested.

4.2. Augmented reality for georeferenced visualization of buried utilities

The underground infrastructure in the U.S. comprises of about 20 million miles of water and wastewater pipes, conduits, and a variety of cables [64,65]. In some locations, major oil and gas pipelines, national defense communication lines, rail and road tunnels also share the underground space. In addition, the demand for new buried utilities is continuously increasing with new construction, and re-construction being fueled by growth as well as aging infrastructure [66]. As a result, excavation contractors are continuously digging and trenching the ground to install new utilities or repair existing lines. Since neither the machines (e.g., backhoes, trenchers, augers) nor their (skilled) operators can "see" what lies buried in their vicinity, utilities are frequently struck and damaged [67].

In the U.S. alone, an underground utility is hit by an excavator every 60 seconds causing billions of dollars in damage each year [68]. Pipeline and Hazardous Materials Safety Administration (PHMSA) statistics from 1990 to 2009 identify excavation damage as the single biggest cause of all reported breakdowns in U.S. pipeline systems, accounting for about 35% of all incidents that cause service interruptions, and jeopardize the safety of workers, bystanders and building occupants. These problems have drawn major attention to research in utility location technologies for both new (e.g., [64]) and existing underground utilities (e.g., [67,69–71]).

Fig. 13. Cabin-mounted display for persistent AR visualization.

Parallel advances in mapping technology also facilitated the adoption of digital geodata archival and distribution methods by utility owners (e.g., [72–75]), and the evolution of standards for characterizing the quality of mapped geodata (e.g., [76]). Widespread recognition of the problem also spawned the national "Call Before You Dig" campaign in 2000 to increase public awareness about using 811, or the One-Call system [77].

Despite these advances, there are some fundamental challenges that make it very difficult for excavator operators to be spatially aware of their surroundings, and thus avoid hitting utility lines while digging. Inaccurate, incomplete, or missing utility location information is often cited as a cause of incidents involving excavators striking buried utilities [64]. The current state of knowledge and the resulting state of practice has two critical limitations when considered from an excavator operator's perspective:

1. *Lack of persistent visual guidance for spatial awareness:* While the practice of marking utility locations on the ground helps in initial excavation planning, such surface markings (e.g., paint, stakes, flags) are the first to be destroyed or dislocated when excavation begins and the top soil or surface is scraped. Thus, excavator operators and field supervisors have no persistent visual clues that can help them be spatially aware of the underground space surrounding an excavator's digging implement. Minor lapses in orientation or in recollecting marked utility locations can thus easily lead to accidents.

2. *Inability to gauge proximity of excavator to buried assets while digging:* Another significant limitation is that an operator has no practical means of knowing the distance of an excavator's digging implement (e.g., bucket) to the nearest buried obstructions until they are exposed. Excavation guidelines in most U.S. states including Michigan require buried utilities to be hand exposed prior to the use of any power equipment [78]. Failure to follow the hand exposure guidelines, which happens often out of ignorance or as a conscious decision, means that the first estimate of proximity an operator receives is when the digging implement actually "touches" a buried utility. It is easy to understand why this first "touch" can often actually be a "strike".

The form of AR visualization most suitable to address this problem is "video-see-through" AR, where a video camera abstracts the user's view, and graphics are registered and superimposed on the video feed to create a continuous AR composite display [79]. In order to achieve this, the line-of-sight (position and orientation) of the video camera must be continuously tracked so that the projection of the superimposed graphics in each frame can be computed relative to the camera's pose. As shown in Fig. 12, using AR visualization, as an excavator digs, the goal is to have superimposed, color-coded geo-data graphics stay "fixed" to their intended ground locations to continuously help orient the operator.

However, in practice, it is not always feasible to have a first-person operator's perspective due to physical encumbrance and potential distractions associated with traditional AR displays (e.g., HMDs). In order to provide a continuous AR display for operator spatial awareness, the most practical approach is to enable AR visualization on a display mounted in the excavator's cabin (Fig. 13). Such a display, when strategically mounted in the operator's field of view may serve as a continuous excavation guidance tool, while providing an unobstructed view of the jobsite.

In order to abstract the operator's viewpoint, a high-speed firewire camera is mounted on the roof of the excavator's cabin. The position of the camera will be continuously tracked using RTK GPS, providing a location uncertainty of 1–2 in. Tracking of the excavator's 3D attitude (heading, pitch, and roll) can be intuitively done using a magnetic orientation sensor. However, the sensor may produce noisy data due to the excavator's metallic construction. In that case, the alternative approach is to use multiple dual antenna RTK GPS receivers. The antennas should be mounted on an excavator's cabin in such a way that their simultaneous position tracking helps interpret a directional vector in 3D space corresponding to the cabin's articulation. A similar idea based on tracking the GPS locations of multiple points on a machine has been attempted before for grade control and blade positioning on bulldozers and graders [80]. Having estimated the location of the viewpoint (i.e., camera) and the orientation of its line-of-sight, a trigonometric 3D registration algorithm is used to compute the pose of the geodata graphics that will be superimposed at each frame to create a composite AR view. Figs. 14–16 show several snapshots corresponding to different steps of the field experiments conducted in this research.

4.3. Augmented reality for collaborative design and information delivery

More recently, AR has drawn more attention in areas such as collaborative design and exchange of information. According to Wang et al. [81], remote collaboration has become an integral aspect of designers' working routine and it is becoming more critical for geographically distributed designers and decision-makers to accurately perceive and comprehend other remote team members' intentions and activities with a high level of awareness and presence as if they were working in the same room. Therefore, it is imperative that the new generation of engineers be equipped with proper understanding and high-level working knowledge of novel tools and technologies that enable them to transcend the traditional boundaries of project design and construction and take advantage of the unmatched benefits of collaborative work and design in diverse environments.

In this regard, attracting and retaining talented students and trainees to science, technology, engineering and mathematics (STEM) disciplines and giving them the opportunity to experience with the latest technologies in educational settings is a crucial first
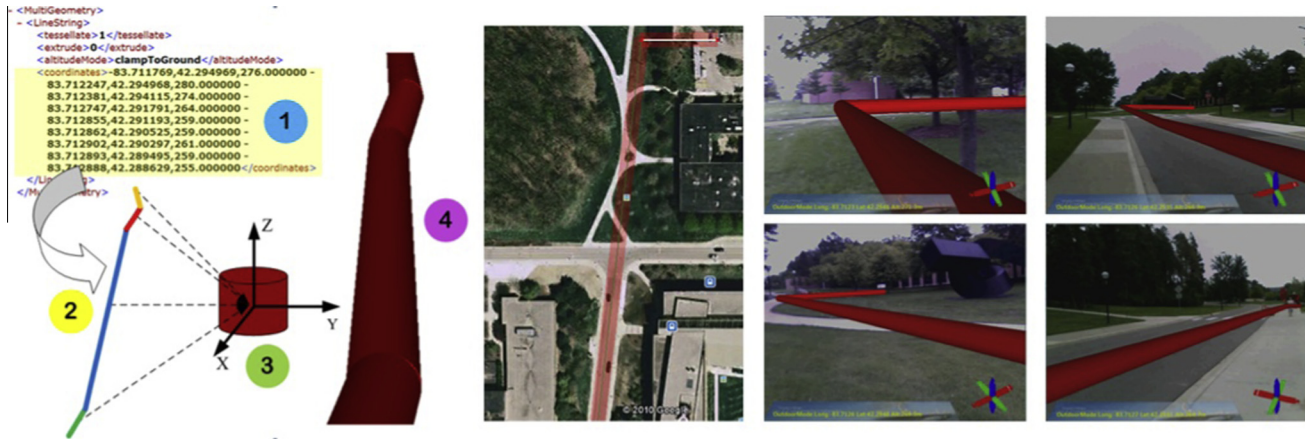
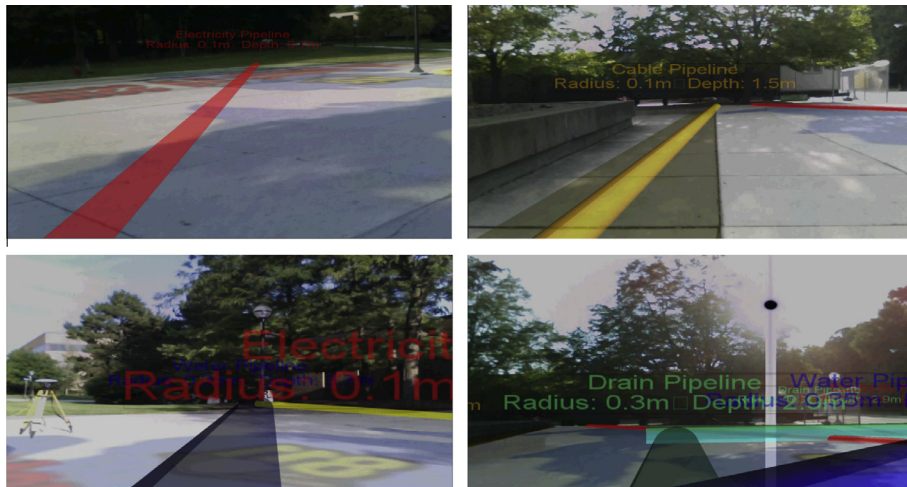**Fig. 14.** Conduit loading procedure, conduits overlaid on Google Earth, and field experiment results.

Fig. 15. Labeling attribute information and color coding of the underground utilities.
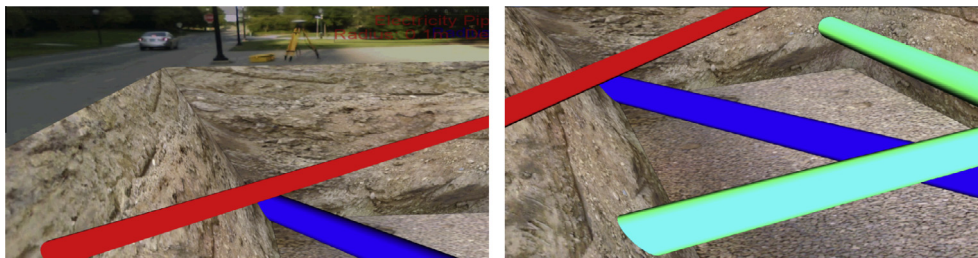

Fig. 16. An X-ray view of the underground utilities.

step. According to the Raytheon STEM Index, a new U.S. News annual index, despite some signs of improvement, student aptitude for and interest in STEM has been mostly flat for more than a decade, even as the need for STEM skills continues to grow. Despite some recent improvements in the number of STEM degrees granted, as a proportion of total degrees granted it still hovers close to the same levels that existed in 2000, indicating that the education pipeline to fill the current and future jobs that will require STEM skills still is not producing enough talent [82].

In particular to construction and civil engineering, research shows that a large percentage of students fail to properly link their classroom learning to real world engineering tasks and the dynamics and complexities involved in a typical construction project

[83–85]. In addition, several academic surveys have indicated that students complain about the limited use of emerging technologies and advanced problem-solving tools in classroom [86]. Engineering students need to also pick up social and technical skills (e.g., critical thinking, decision making, collaboration, and leadership) that they need in order to be competent in the digital age.

One of the fastest emerging technologies in collaborative engineering education, training, and design is visualization. Currently, there are major gaps between research advancements in visualization and the integration of visualization techniques in pedagogical and engineering settings, as well as outstanding implementation challenges that need to be properly addressed. This Subsection describes the latest work by the authors in using AR as an
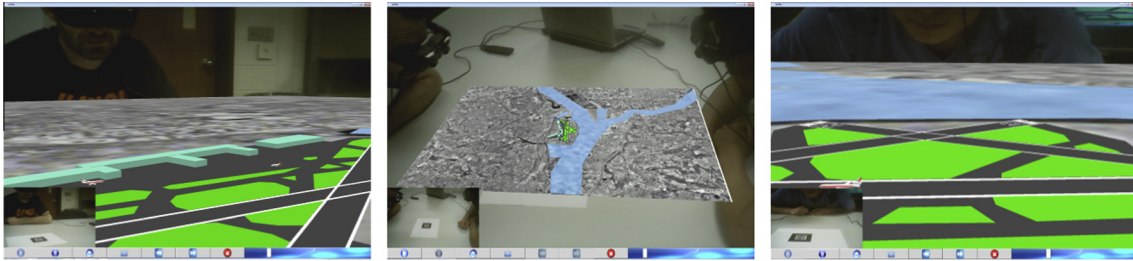
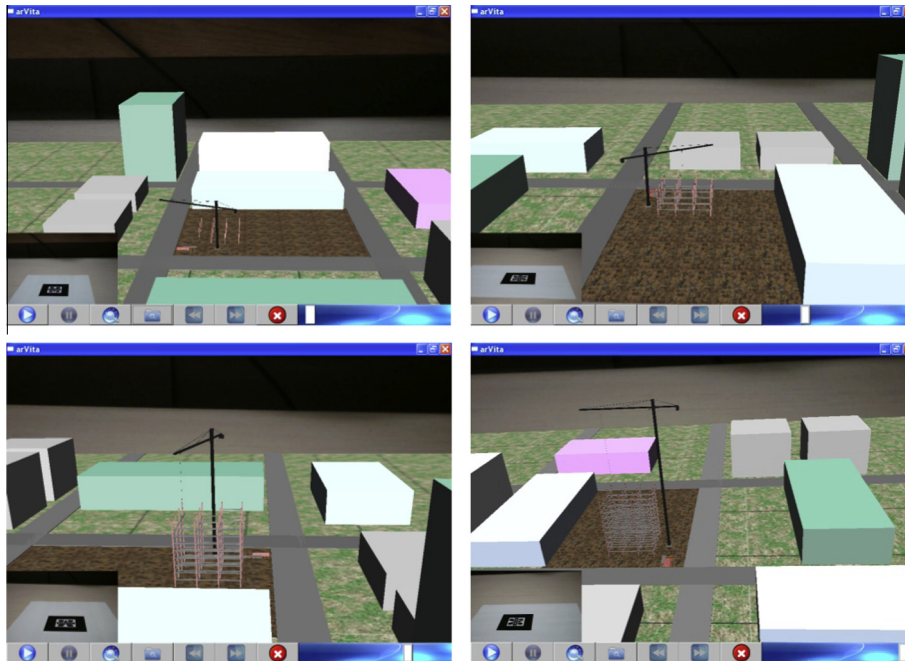**Fig. 17.** Two users are observing the animation lying on the table.

Fig. 18. Steel erection activities at different timestamps.

interconnecting media to bridge the gap between computer-based dynamic visualization and paper-based collaboratively-shared workspace. Collaborative AR environments allow users to work across the table face-to-face, shift the focus of shared workspace instantly, and jointly analyze dynamic engineering scenarios. This idea is developed and implemented in ARVita (acronym for Augmented Reality Vitascope), in which multiple users wearing HMDs can observe and interact with dynamic simulated construction activities laid on the surface of a table [87].

Compared to VR, AR can enhance the traditional learning experience since:

1. The ability to learn concepts and ideas through interacting with a scene and building one's own knowledge (constructivism learning) facilitates the generation of knowledge and skills that could otherwise take too long to accumulate.
2. Traditional methods of learning spatially relate content by viewing 2D diagrams or images create a cognitive filter. This filter exists even when working with 3D objects on a computer screen because the manipulation of objects in space is done through mouse clicks. By using 3D immersive AR, a more direct cognitive path toward understanding the content is possible.
3. Making mistakes during the learning process will have literally no real consequence for the educator, whereas in traditional learning, failure to follow certain rules or precautions while operating machinery or handling a hazardous material could lead to serious safety and health-related problems.

4. AR supports discovery-based learning, an instructional technique in which students take control of their own learning process, acquire information, and use that information in order to experience scenarios that may not be feasible in reality given the time and space constraints of a typical engineering project.
5. By providing multiple students with access to a shared augmented space populated with real and virtual objects, they are encouraged to become involved in teamwork and brainstorming activities to solve a problem, which simultaneously helps them improve their communication and social interaction skills.

The motivation behind ARVita is to allow multiple users to observe the animation from different perspectives, and promptly shift the focus of the shared working space in a natural approach. As shown in Fig. 17, these natural interactions include rotating the marker to find vantage points, and pointing at the model to attract others' attention. Given that the scale of the model may prevent users from getting close enough to interesting regions, ARVita provides users with basic zooming and panning functionalities.

The focus of the shared working space cannot only be switched spatially, but also temporally. Users can choose to observe the animation at different speeds, or jump instantaneously along the timeline (Fig. 18).

The current version of ARVita software and its source code can be found on the website: <http://live.engin.umich.edu/software.htm>.

5. Conclusions and directions for future work

In AEC applications, the requirement of blending synthetic and physical objects distinguishes AR from other visualization technologies in three aspects:

1. It reinforces the connections between people and objects, and promotes engineers' appreciation about their working context.
2. It allows engineers to perform field tasks with the awareness of both the physical and synthetic environments.
3. It offsets the significant cost of 3D Model Engineering by including the real world background.

This paper reviewed critical problems in AR and investigated technical approaches to address the fundamental challenges that prevent the technology from being usefully deployed in AEC applications, such as the alignment of virtual objects with the real environment continuously across time and space (spatial registration), blending of virtual entities with their real background faithfully to create a sustained illusion of co-existence (visual occlusion), and the integration of these methods to a scalable and extensible computing AR framework that is openly accessible to the teaching and research community. The research findings have been evaluated in several challenging AEC applications where the potential of having a significant economic and social impact is high. Examples of validation test beds implemented include:

1. An AR post-disaster reconnaissance framework that enables building inspectors to rapidly evaluate and quantify structural damage sustained by buildings in seismic events such as earthquakes or blasts.
2. An AR visual excavator-utility collision avoidance system that enables workers to "see" buried utilities hidden underground, thus helping prevent accidental utility strikes.
3. A tabletop collaborative AR visualization framework that allows multiple users to observe and interact with visual simulations of engineering processes.

In addition to the key challenges and application areas presented in this paper, some directions for future work include addressing practical challenges related to mobile field implementation such as mobility and ergonomics requirements (i.e., user comfort), power limitations, ruggedness (ability to function in chaotic and harsh environments), robust image registration for outdoor uncontrolled conditions (i.e., synchronizing the captured image and sensor measurements), filtering ambient noise and data interferences, optimizing the adaptive latency compensation algorithm with image processing techniques, and adding more interactivity features to the AR interface (e.g., providing an AR user with the ability to connect to a remote server and update project information and progress status in real-time through the AR interface).

Acknowledgments

References

[1] F.P. Brooks, What's real about virtual reality?, J Comput. Graph. Appl. 19 (6) (1999) 16–27.
[2] R. Azuma, Y. Baillot, R. Behringer, S. Feiner, S. Julier, B. Malntyre, Recent advances in augmented reality, J. Comput. Graph. Appl. (2001) 34–47.
[3] R. Azuma, A survey of augmented reality, Teleoper. Virtual Environ. (1997) 355–385.
[4] A.H. Behzdan, V.R. Kamat, Visualization of construction graphics in outdoor augmented reality, in: Proceedings of the Winter Simulation Conference, Institute of Electrical and Electronics Engineers (IEEE), Orlando, FL, 2005.
[5] P. Milgram, F. Kishino, A taxonomy of mixed reality visual displays, IEICE Trans. Inform. Syst. E77-D (12) (1994) 1321–1329.
[6] S. Rankohi, L. Waugh, Review and analysis of augmented reality literature for construction industry, J. Visual. Eng. (2013) 1–9.
[7] D.H. Shin, P.S. Dunston, Identification of application areas for augmented reality in industrial construction based on technology suitability, J. Autom. Constr. 17 (7) (2008) 882–894.
[8] A.H. Behzdan, ARVISCOPE: Georeferenced Visualization of Dynamic Construction Processes in Three-Dimensional Outdoor Augmented Reality, Ph.D. Dissertation, Department of Civil and Environmental Engineering, University of Michigan, Ann Arbor, MI, 2008.
[9] G. Roberts, A. Evans, A.H. Dodson, B. Denby, S. Cooper, R. Hollands, The use of augmented reality, GPS and INS for subsurface data visualization, in: Proceedings of the FIG XIII International Congress, 2002, pp. 1–12.
[10] A.H. Behzdan, V.R. Kamat, Interactive augmented reality visualization for improved damage prevention and maintenance of underground infrastructure, Proceedings of Construction Research Congress, American Society of Civil Engineers, Seattle, WA, 2009.
[11] G. Schall, J. Sebastian, D. Schmalstieg, VIDENTE – 3D visualization of underground infrastructure using handheld augmented reality, GeoHydroinformatics: Integrating GIS and Water Engineering (2010).
[12] A. Webster, S. Feiner, B. Macintyre, W. Massie, Augmented reality in architectural construction, inspection, and renovation, in: Proceedings of ASCE Congress on Computing in Civil Engineering, 1996, p. 12.
[13] P. Georgel, P. Schroeder, S. Benhimane, S. Hinterstoisser, An industrial augmented reality solution for discrepancy check, in: Proceedings of the IEEE and ACM International Symposium on Mixed and Augmented Reality, 2007.
[14] M. Golparvar-Fard, F. Pena-Mora, C.A. Arboleda, S. Lee, Visualization of construction progress monitoring with 4D simulation model overlaid on time-lapsed photographs, J. Comput. Civ. Eng. 23 (6) (2009) 391–404.
[15] F. Dai, M. Lu, V.R. Kamat, Analytical approach to augmenting site photos with 3D graphics of underground infrastructure in construction engineering applications, J. Comput. Civ. Eng. 25 (1) (2011) 66–74.
[16] A.H. Behzdan, V.R. Kamat, Georeferenced registration of construction graphics in mobile outdoor augmented reality, J. Comput. Civ. Eng. 21 (4) (2007) 247–258.
[17] B. Thomas, W. Piekarski, B. Gunther, Using augmented reality to visualise architecture designs in an outdoor environment, Int. J. Des. Comput.: Spec. Iss. Des. Comput. Net. (1999).
[18] D. Aiteanu, B. Hiller, A. Graser, A step forward in manual welding: demonstration of augmented reality helmet, in: Proceedings of the IEEE and ACM International Symposium on Mixed and Augmented Reality, 2003.
[19] V. Kamat, J. Martinez, M. Fischer, M. Golparvar-Fard, F. Peña-Mora, S. Savarese, Research in visualization techniques for field construction, J. Constr. Eng. Manage. Spec. Iss.: Constr. Eng.: Opportunity Vision Educ. Pract. Res. 137 (10) (2011) 853–862.
[20] M. Golparvar-Fard, F. Peña-Mora, S. Savarese, D4AR-A 4-dimensional augmented reality model for automating construction progress data collection, processing and communication, J. Inform. Technol. Constr. (ITcon) 14 (2009) 129–153.
[21] K. Karsch, M. Golparvar-Fard, D. Forsyth, ConstructAide: analyzing and visualizing construction sites through photographs and building models, in: Proceedings of ACM Transactions on Graphics (SIGGRAPH Asia), Shenzhen, China, 2014.
[22] C. Woodward, M. Hakkarainen, M. Billinghurst, A client/server architecture for augmented reality on mobile phones, in: P. Alencar, D. Cowan (Eds.), Handbook of Research on Mobile Software Engineering – Design, Implementation and Emergent Applications, vol. I, Engineering Science Reference, 2012, pp. 1–16.
[23] X. Wang, P.S. Dunston, Tangible mixed reality for remote design review: a study understanding user perception and acceptance, J. Visual. Eng. (2013) 1–8.
[24] S. Siltanen, V. Oksman, M. Ainasoja, User-centered design of augmented reality interior design service, Int. J. Arts Sci. 6 (1) (2013) 547–563.
[25] A.M. Malkawi, R.S. Srinivasan, A new paradigm for human-building interaction: the use of CFD and augmented reality, J. Autom. Constr. 14 (1) (2004) 71–84.
[26] R. Lakaemper, A.M. Malkawi, Integrating robot mapping and augmented building simulation, J. Comput. Civ. Eng. 23 (6) (2009) 384–390.
[27] S. Dong, A.H. Behzdan, C. Feng, V.R. Kamat, Collaborative visualization of engineering processes using tabletop augmented reality, vol. 55, Elsevier Journal of Advances in Engineering Software, New York, NY, 2013. pp. 45–55.

[28] A. Shirazi, A.H. Behzadan, Design and assessment of a mobile augmented reality-based information delivery tool for construction and civil engineering curriculum, J. Prof. Iss. Eng. Educ. Pract. (2014). 04014012 (published online).

[29] S.A. Talmaki, V.R. Kamat, H. Cai, Geometric modeling of geospatial data for visualization-assisted excavation, Adv. Eng. Inform. 27 (2) (2013) 283–298 (Elsevier Science, New York, NY).

[30] S. Dong, Scalable and Extensible Augmented Reality with Applications in Civil Infrastructure Systems, Ph.D. Dissertation, Department of Civil and Environmental Engineering, University of Michigan, Ann Arbor, MI, 2012.

[31] A.H. Behzadan, V.R. Kamat, Automated generation of operations level construction animations in outdoor augmented reality, J. Comput. Civ. Eng. 23 (6) (2009) 405–417.

[32] D. Shreiner, M. Woo, J. Neider, T. Davis, OpenGL Programming Guide, Pearson Education (2006).

[33] P. Martz, OpenSceneGraph Quick Start Guide, 2007.

[34] T. Vincenty, Direct and inverse solutions of geodesics on the ellipsoid with application of nested equations, Surv. Rev. (1975).

[35] A.H. Behzadan, V.R. Kamat, Resolving incorrect occlusion in augmented reality animations of simulated construction operations, in: Proceedings of the 15th Annual Workshop of the European Group for Intelligent Computing in Engineering (EG-ICE), European Group for Intelligent Computing in Engineering, Plymouth, UK, 2008.

[36] M.M. Wloka, B.G. Anderson, Resolving occlusion in augmented reality, in: Proceedings of Symposium on Interactive 3D Graphics, Monterey, CA, 1995.

[37] M.-O. Berger, Resolving occlusion in augmented reality: a contour based approach without 3D reconstruction, in: Proceedings of IEEE Conference on Computer Vision and Pattern Recognition, 1997.

[38] V. Lepetit, M.-O. Berger, A semi-automatic method for resolving occlusion in augmented reality, in: Proceedings of IEEE Conference on Computer Vision and Pattern Recognition, 2000.

[39] P.-A. Fortin, P. Hebert, Handling occlusions in real-time augmented reality: dealing with movable real and virtual objects, in: Proceedings of the Canadian Conference on Computer and Robot Vision, 2006, pp. 54–62.

[40] S.-W. Ryu, J.-H. Han, J. Jeong, S.H. Lee, J.I. Park, Real-time occlusion culling for augmented reality, in: Proceedings of the Korea–Japan Joint Workshop on Frontiers of Computer Vision, 2010, p. 12.

[41] J. Louis, J. Martinez, Rendering stereoscopic augmented reality scenes with occlusions using depth from stereo and texture mapping, in: Proceedings of the Construction Research Congress, West Lafayette, IN, 2012.

[42] Y. Tian, T. Guan, C. Wang, Real-time occlusion handling in augmented reality based on an object tracking approach, Sensors 10 (2010) 2885–2900.

[43] R. Koch, I. Schiller, B. Bartczak, F. Kellner, K. Koser, MixIn3D: 3D mixed reality with ToF-Camera, in: Proceedings of DAGM Workshop on Dynamic 3D Imaging, Jena, Germany, 2009.

[44] C. Beder, B. Bartczak, R. Koch, A comparison of PMD-cameras and stereo-vision for the task of surface reconstruction using patchlets, in: Proceedings of IEEE Conference on Computer Vision and Pattern Recognition, 2007.

[45] B.S. Gokturk, H. Yalcin, C. Bamji, A time-of-flight depth sensor – system description, issues and solutions, in: Proceedings of IEEE Conference on Computer Vision and Pattern Recognition Workshop, 2010.

[46] M. Lourakis, homest: A C/C++ Library for Robust, Non-linear Homography Estimation. <http://www.ics.forth.gr/~lourakis/homest/>, 2011.

[47] S. Côté, P. Trudel, R. Snyder, R. Gervais, An augmented reality tool for facilitating on-site interpretation of 2D construction drawings, in: Proceedings of the 13th International Conference on Construction Applications of Virtual Reality (CONVR), London, UK, 2013.

[48] S. Dong, V.R. Kamat, SMART: scalable and modular augmented reality template for rapid development of engineering visualization applications, J. Visual. Eng. 1 (1) (2013) 1–17 (Springer, London, UK).

[49] A.H. Behzadan, B.W. Timm, V.R. Kamat, General-purpose modular hardware and software framework for mobile outdoor augmented reality applications in engineering, Adv. Eng. Inform. 22 (1) (2008) 90–105.

[50] C. Rojah, ATC-20-1 Field Manual: Postearthquake Safety Evaluation of Buildings, Applied Technology Council, 2005. p. 12.

[51] G. Chock, ATC-20 Post-Earthquake Building Safety Evaluations Performed after the October 15, 2006 Hawaii Earthquakes Summary and Recommendations for Improvements (updated), Hawaii Structural Engineers Association, 2013.

[52] F. Vidal, M. Feriche, A. Ontiveros, Basic techniques for quick and rapid post-earthquake assessments of building safety, in: Proceedings of the International Workshop on Seismic Microzoning and Risk Reduction, Almeria, Spain, 2009.

[53] S.K. Tubbesing, The Loma Prieta, California, Earthquake of October 17, 1989-Loss Estimation and Procedures, in: S.K. Tubbesing (Ed.), USGS Professional Paper: 1553-A, U.S. Geological Survey, 1994.

[54] V.R. Kamat, S. El-Tawil, Evaluation of augmented reality for rapid assessment of earthquake-induced building damage, J. Comput. Civ. Eng. 21 (5) (2007) 303–310.

[55] E. Miranda, M. Asce, S.D. Akkar, Generalized interstory drift spectrum, J. Struct. Eng. 132 (6) (2006) 840–852.

[56] S. Krishnan, Case studies of damage to tall steel moment-frame buildings in Southern California during large San Andreas earthquakes, Bull. Seismol. Soc. Am. 96 (4A) (2006) 1523–1537.

[57] D.A. Skolnik, J.W. Wallace, Critical assessment of interstory drift measurements, J. Struct. Eng. 136 (12) (2010) 1574–1584.

[58] A.M. Wahbeh, J.P. Caffrey, S.F. Masri, A vision-based approach for the direct measurement of displacements in vibrating systems, Smart Mater. Struct. 12 (5) (2003) 785–794.

[59] Y. Ji, A computer vision-based approach for structural displacement measurement, Sens. Smart Struct. Technol. Civ. Mech. Aerospace Syst. 43 (7) (2010) 642–647.

[60] Y. Fukuda, M. Feng, Y. Narita, S. Kaneko, T. Tanaka, Vision-based displacement sensor for monitoring dynamic response using robust object search algorithm, IEEE Sensors 13 (12) (2013) 4725–4732.

[61] M. Alba, L. Fregonese, F. Prandi, M. Scaioni, P. Valgoi, Structural monitoring of a large dam by terrestrial laser, in: Proceedings of the ISPRS Commission Symposium, Dresden, Germany, 2006.

[62] H.S. Park, H.M. Lee, H. Adeli, I. Lee, A new approach for health monitoring of structures: terrestrial laser scanning, J. Comput. Aided Civ. Infrastruct. Eng. 22 (1) (2007) 19–30.

[63] S. Dong, V.R. Kamat, Robust mobile computing framework for visualization of simulated processes in augmented reality, in: Proceedings of the Winter Simulation Conference, Baltimore, MD, 2010.

[64] A. Patel, A. Chasey, S.T. Ariaratnam, Integrating global positioning system with laser technology to capture as-built information during open-cut construction, J. Pipeline Syst. Eng. Pract. 1 (4) (2010) 147–155.

[65] R. Sterling, Utility Locating Technologies: A Summary of Responses to a Statement of Need Distributed by the Federal Laboratory Consortium for Technology Transfer, Federal Laboratory Consortium Special Reports Series No. 9, Louisiana Tech University, Ruston, LA, 2000.

[66] EPA, United States Environmental Protection Agency, Drinking Water Needs Survey and Assessment, Fourth Report to Congress. <http://www.epa.gov/safewater/needssurvey/pdfs/2007/report_needssurvey_2007.pdf>, 2007 (accessed 14.09.10).

[67] J. Lester, L.E. Bernold, Innovative process to characterize buried utilities using ground penetrating radar, Autom. Constr. 16 (4) (2007) 546–555.

[68] J.T. Spurgin, J. Lopez, K. Kerr, Utility damage prevention – what can your agency do?, Proceedings of the APWA International Public Works Congress & Exposition, American Public Works Association (APWA), Kansas City, MO, 2009

[69] Underground Imaging Technologies (UIT), Seeing What Can't Be Seen with 3D Subsurface Imaging. <www.uit-systems.com>, 2010 (accessed 10.02.11).

[70] Virtual Underground (VUG), Virtual Underground. <http://www.virtualug.com>, 2010 (accessed 10.02.11).

[71] Subsurface Imaging Systems (SIS), Surface penetrating radar systems. <http://subsurfaceimagingsystems.com>, 2011 (accessed 10.02.11).

[72] ESRI, DTE Energy, Energy Currents – GIS for Energy, Spring 2005, Redlands, CA. <http://www.esri.com/library/reprints/pdfs/enercur-dte-energy.pdf>, 2005 (accessed 15.09.10).

[73] Underground Imaging Technologies (UIT), Case Studies, <http://www.uit-systems.com/case_studies.html>, 2009 (accessed 10.02.11).

[74] J. Wyland, Rio Grande Electric Moves Mapping and Field Work into Digital Realm, PRWeb, February 12, 2009. <http://www.prweb.com/releases/mapping/utility/prweb2027014.htm>, 2009 (accessed 10.02.11).

[75] T.R. Porter, Navigation Sensors Enhance GIS Capabilities, Pipeline and Gas Technology, July 1, 2010. <http://www.pipelineandgastechnology.com/Operations/SCADAAutomation/item63959.php>, 2010 (accessed 10.02.11).

[76] ASCE (American Society of Civil Engineers), Standard Guideline for the Collection and Depiction of Existing Subsurface Utility Data, ASCE/CI Standard 38-02, Reston, VA, 2002.

[77] Common Ground Alliance (CGA), 811 Campaign. <http://www.call811.com/>, 2010 (accessed 15.09.10).

[78] MISS DIG Systems Inc. (MDS), One-Call Excavation Handbook. <http://www.missdig.net/images/Education_items/2007onecall_handbook.pdf> (accessed 15.09.11).

[79] M. Kanbara, T. Okuma, H. Takemura, N. Yokoya, A stereoscopic video see-through augmented reality system based on real-time vision-based registration, in: Proceedings of IEEE Virtual Reality, New Brunswick, NJ, 2000.

[80] G. Roberts, O. Ogundipe, A.H. Dodson, Construction plant control using RTK GPS, in: Proceedings of the FIG XXII International Congress, Washington, DC, 2002.

[81] X. Wang, P.E.D. Love, M.J. Kim, W. Wang, Mutual awareness in collaborative design: an augmented reality integrated telepresence system, J. Comput. Ind. 65 (2) (2014) 314–324.

[82] L. Alphonse, New STEM Index Finds America's STEM Talent Pool Still Too Shallow to Meet Demand, U.S. News. <http://www.usnews.com/news/stem-index/articles/2014/04/23/new-stem-index-finds-americas-stem-talent-pool-still-too-shallow-to-meet-demand?int=9a5208>, 2014.

[83] D. Arditi, G. Polat, Graduate education in construction management, J. Prof. Iss. Eng. Educ. Pract. 136 (3) (2010) 175–179.

[84] J. Bowie, Enhancing Classroom Instruction with Collaborative Technologies. <http://www.eschoolnews.com/2010/12/20/enhancing-classroom-instruction-with-collaborative-technologies/>, 2010.

[85] J.E. Mills, D.F. Treagust, Engineering education – is problem-based or project-based learning the answer?, Aust J. Eng. Educ. (2003) 1–16.

[86] A. Behzadan, R.V. Kamat, A framework for utilizing context-aware augmented reality visualization in engineering education, in: Proceedings of the International Conference on Construction Applications of Virtual Reality (CONVR), Taipei, Taiwan, 2012.

[87] S. Dong, V.R. Kamat, Collaborative visualization of simulated processes using tabletop fiducial augmented reality, in: Proceedings of the Winter Simulation Conference, Phoenix, AZ, 2011.